α-spectroscopy studies of the new nuclides ^{165}Pt and ^{170}Hg

J. Hilton,[1,2,*] J. Uusitalo,[1] J. Sarén,[1] R. D. Page,[2] D. T. Joss,[2] M. A. M. AlAqeel,[2,3] H. Badran,[1] A. D. Briscoe,[2] T. Calverley,[1,2] D. M. Cox,[1,†] T. Grahn,[1] A. Gredley,[2] P. T. Greenlees,[1] R. Harding,[4] A. Herzan,[5,2,‡] E. Higgins,[2] R. Julin,[1] S. Juutinen,[1] J. Konki,[1,§] M. Labiche,[6] M. Leino,[1] M. C. Lewis,[2] J. Ojala,[1] J. Pakarinen,[1] P. Papadakis,[1,‖] J. Partanen,[1,¶] P. Rahkila,[1] P. Ruotsalainen,[1] M. Sandzelius,[1] C. Scholey,[1] J. Sorri,[1,7] L. Sottili,[1] S. Stolze,[1,**] and F. Wearing[2]

[1]*University of Jyvaskyla, Department of Physics, P.O. Box 35, FI-40014 University of Jyvaskyla, Finland*

[2]*University of Liverpool, Oliver Lodge Laboratory, Liverpool L69 7ZE, United Kingdom*

[3]*Imam Mohammad Ibn Saud Islamic University (IMISU), Riyadh, 11623, Saudi Arabia*

[4]*University of York, Heslington, York YO10 5DD, United Kingdom*

[5]*Institute of Physics, Slovak Academy of Science, Bratislava SK-84511, Slovakia*

[6]*STFC Daresbury Laboratory, Sci-Tech Daresbury, Warrington WA4 4AD, United Kingdom*

[7]*Sodankylä Geophysical Observatory, University of Oulu, FI-99600 Sodankylä, Finland*

(Received 13 May 2019; published 8 July 2019)

The new nuclides ^{165}Pt and ^{170}Hg were produced in the reactions ^{92}Mo(^{78}Kr, $5n$) and ^{96}Ru(^{78}Kr, $4n$) at bombarding energies of 418 MeV and 390 MeV, respectively. For ^{170}Hg an α-particle energy of $E_\alpha = 7590(30)$ keV and half-life of $t_{1/2} = 0.08^{+0.40}_{-0.04}$ ms were deduced, while for ^{165}Pt the corresponding values were 7272(14) keV and $0.26^{+0.26}_{-0.09}$ ms. Comparison of the reduced α-decay widths with systematics indicates that both α decays are unhindered. Although combining the measured α-decay Q values with extrapolated masses suggests that both new nuclides are unbound to two-proton emission by more than 1 MeV, their α-decay half-lives are too short for this decay mode to compete. Improved data were also obtained for ^{166,167}Pt, produced via the ^{96}Ru(^{78}Kr, $\alpha 4n$) and ^{96}Ru(^{78}Kr, $\alpha 3n$) reactions at bombarding energies of 390 MeV and 418 MeV.

DOI: 10.1103/PhysRevC.100.014305

I. INTRODUCTION

Investigating exotic nuclei at the proton drip line is a very challenging process. The lightest isotopes of heavy elements often have extremely small production cross sections and in order to study them it is essential to employ efficient and selective techniques. The main challenge then arises from the short half-lives, which decrease dramatically for nuclei close to the proton drip line [1]. One common technique used to study such nuclei is the combination of an in-flight separator with a fast and efficient decay spectrometer capable of resolving the proton and α-particle energies of different reaction products. By separating and transporting short-lived nuclei to a focal plane equipped accordingly in only a few hundred nanoseconds, decay spectroscopy can be undertaken on nuclei with microsecond lifetimes.

Measurement of the α-particle energy and half-life allows calculation of the reduced α-decay width, which can assist in assigning the spins and parities of the states involved. Decay Q values also allow testing and potential refinement of theoretical mass models. Systematic studies of these properties can give insights into how magic numbers and other shell effects evolve far from β stability.

In this work, the new MARA (mass analysing recoil apparatus) vacuum mode recoil mass separator [2,3] was used to investigate neutron-deficient isotopes of Pt and Hg. Until now, the lightest known isotopes of platinum were ^{166,167}Pt with measured α-particle energies of $E_\alpha = 7110(15)$ keV, 6988(10) keV and half-lives of $t_{1/2} = 0.3(1)$ ms, 0.7(2) ms for ^{166}Pt and ^{167}Pt, respectively [4]. The previous lightest known isotope of mercury was ^{171}Hg, for which values of $E_\alpha = 7488(12)$ keV and $t_{1/2} = 59^{+36}_{-16}\,\mu$s were reported [5]. The present work improves upon the previous Pt results with more precise measurements of both energy and half-life in addition to presenting the identification and measurements of the α-decay properties of the new nuclides ^{165}Pt and ^{170}Hg.

II. EXPERIMENTAL DETAILS

This work uses data from separate experiments conducted using MARA at the University of Jyväskylä, Finland. The K130 cyclotron was used to produce beams of ^{78}Kr^{15+} ions that bombarded ^{92}Mo and ^{96}Ru targets, resulting in three data sets shown in Table I.

*joshua.b.hilton@jyu.fi

†Present address: Department of Physics, Lund University, S-22100 Lund, Sweden.

‡Present Address: Institute of Physics, Slovak Academy of Science, Bratislava, SK-84511, Slovakia.

§Present address: CERN, CH-1211 Geneva 23, Switzerland.

‖Present address: University of Liverpool, Oliver Lodge Laboratory, Liverpool L69 7ZE, United Kingdom.

¶Deceased.

**Present address: Physics Division, Argonne National Laboratory, 9700 South Cass Avenue, Lemont, Illinois 60439, USA.

TABLE I. The beam energies, targets, and irradiation times for the data sets collected during this work. In all cases, the incident beam was ^{78}Kr and the specified beam energy was measured upstream of the target. The target thicknesses provided are the nominal values from when the target foils were manufactured.

Beam energy (MeV)	Target	Target thickness (μg/cm^2)	Irradiation time (h)	Data set
418(4)	^{92}Mo	500	67	A
418(4)	^{96}Ru	170	257	B
390(4)	^{96}Ru	170	179	C

The ^{96}Ru target was a foil of 96.5% isotopic enrichment supported by a 60 μg/cm^2 thick layer of carbon. The target was mounted so that the carbon layer was upstream of the ^{96}Ru material. The ^{92}Mo target was a self-supporting foil of ≈97% isotopic enrichment. The average beam intensity was 12 pnA for data sets A and B, and 5 pnA for data set C. The electric and magnetic fields of MARA for data sets A, B, and C were chosen to optimize the transmission of ^{165}Pt, ^{169}Au, and ^{170}Hg ions, respectively. In the present work, the flight time of recoiling nuclei through MARA was calculated to be ≈600 ns.

Fusion-evaporation reaction products ("recoils") transported to the focal plane of MARA passed through a multiwire proportional counter (MWPC) before being implanted into a double-sided silicon strip detector (DSSD). Two different designs of DSSD were used in this work, both with a nominal thickness of 300 μm. The DSSD used for data sets A and B had 128 vertical strips on one face and 48 horizontal on the other. The strip pitch was 1 mm on both faces and the full width at half-maximum (FWHM) measured for the ^{169}Pt α-decay line ($E_\alpha = 6678(15)$ keV [6]) was 40 keV. The DSSD used for data set C had a strip pitch of 0.67 mm, with 192 vertical and 72 horizontal strips on its two faces. Using this DSSD a FWHM of 33 keV was measured for the ^{155}Lu^m α-decay ($E_\alpha = 7390(5)$ keV [7]) line.

The MWPC comprised a grid of 20 μm diameter gold-coated tungsten wires with 1 mm spacing in 3.5 mbar flowing isobutane gas and provided spatial information on the recoils, which were dispersed across the MARA focal plane according to the ratio of their mass number (A) and charge (Q). This can be seen in Fig. 1, which shows two-dimensional spectra of the A/Q ratio of the recoils versus the energy of subsequent α particles in the same DSSD pixel. Combining information on the time of flight of the recoils between the MWPC and the DSSD with the energy measured in the DSSD allowed recoils to be distinguished from other implanted ions. Two 500 μm thick silicon detectors were mounted adjacently behind the DSSD to identify light ions that punched through the DSSD. Signals observed in the DSSD without a coincident signal in these silicon detectors or in the MWPC were assumed to be from radioactive decays of implanted nuclei.

All detector signals were time stamped by a global 100 MHz clock to allow both temporal and spatial correlations

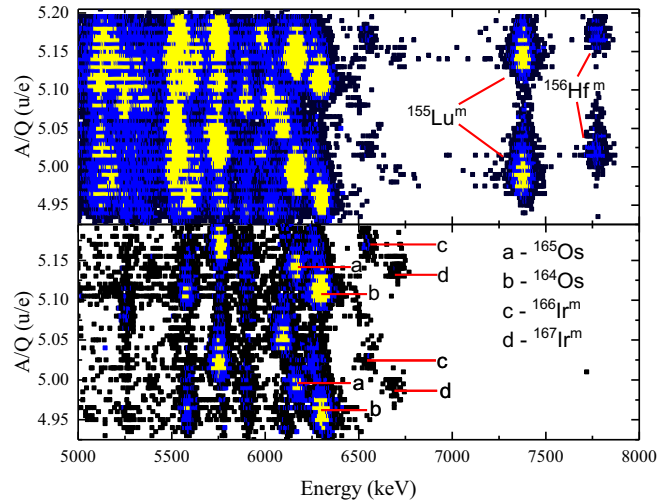

FIG. 1. The upper panel shows the distribution of the energies of α particles occurring within 10 ms of a recoil being implanted into the same DSSD pixel plotted against the ratio of the mass number to charge state (A/Q) of the recoil at the MWPC. The lower panel shows the α-particle energy spectrum of decays occurring within 10 ms of the recoil that are followed by another α particle within 50 ms versus the A/Q of the recoil. The plots present the part of data set A that was used to calibrate the A/Q distribution for the experiment and show that two charge states were collected for each labeled nuclide. The color scale in both panels is set such that black points represent 2–4 events, blue points 5–24 events, and yellow points ⩾ 25 events.

to be made between recoils and subsequent radioactive decays within the full detector array [8]. The data were analyzed with the GRAIN software package [9] and with analysis code written in the Python programming language.

III. RESULTS AND DISCUSSION

A. Decay of ^{165}Pt

The dominant radioactive decay mode of the ground state of ^{165}Pt is expected to be α-particle emission [12]. As shown in Fig. 2, the daughter of the α decay of ^{165}Pt is ^{161}Os, which was first identified by Bianco *et al.* who reported an α-particle energy of 6890(12) keV and half-life of 0.64(6) ms [13]. The α-decay daughter of ^{161}Os, ^{157}W, undergoes β decay with a half-life of 275(40) ms. These β decays indirectly populate low-lying states in ^{157}Ta, which in turn undergo α decay with α-particle energies of 6117(4) keV and 6213(4) keV and half-lives of 10.1(4) ms and 4.3(1) ms [7,14].

Data set A was searched for α decays of ^{165}Pt followed in the same DSSD pixel by event sequences consistent with the decay chain of its daughter ^{161}Os, and four chains were found. Figure 3(a) shows the correlation plot of mother decays that occurred within 10 ms of recoil implantation plotted against the energies of daughter decays that occurred within a further 50 ms. Three correlated event chains can be seen where the daughter energy is consistent with that reported for ^{161}Os. The mean lifetime for the daughter decays is consistent within errors with that of ^{161}Os.

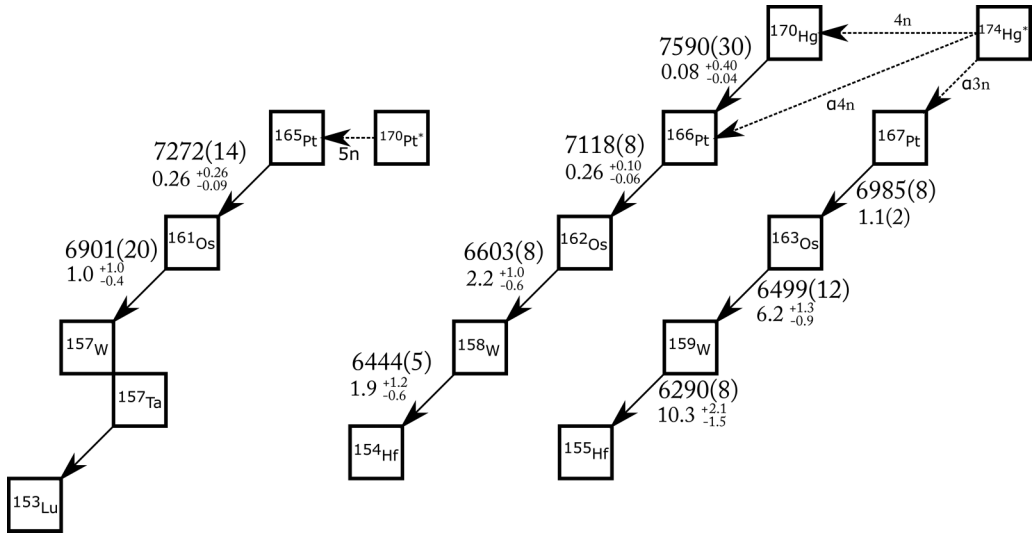

FIG. 2. The decay chains of the nuclides of interest. α-particle energies are labeled in keV and indicated by solid arrows. Half-lives are labeled in ms, and all values are those measured in the present work. The dashed arrows denote fusion-evaporation channels used to produce ^{165,166,167}Pt and ^{170}Hg.

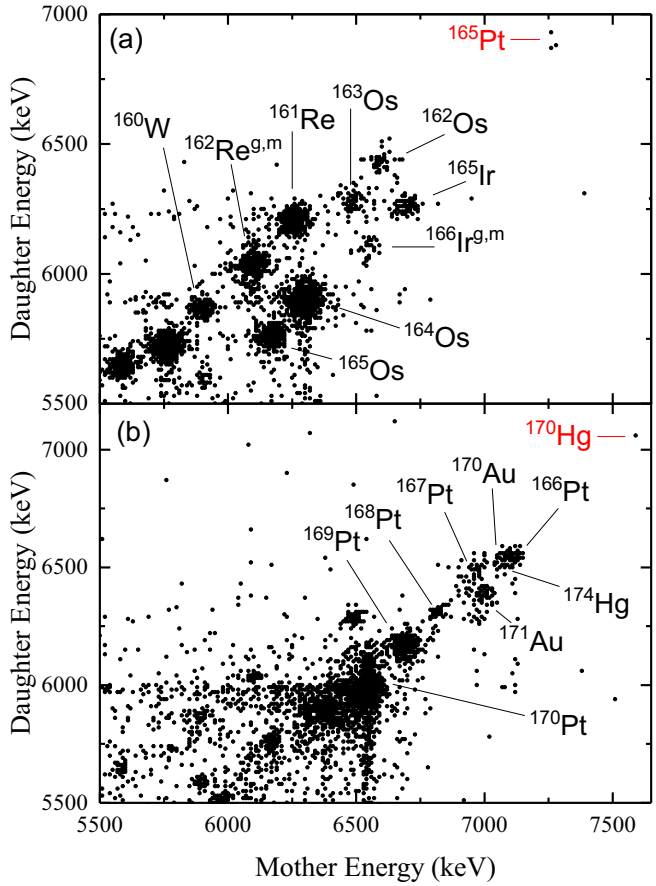

FIG. 3. Two-dimensional spectra of α-particle energies of mother decays occurring within 10 ms of a recoil being implanted into the same DSSD pixel plotted against those of subsequent daughter α decays occurring (a) within 50 ms from data set A, and (b) within 100 ms from data set C. Selected correlated mother α decays are labeled, with newly identified nuclides highlighted in red.

Analysis of the grand-daughter decays for these event chains presented in Table III reveals that for the first two the energy is consistent with it being an α decay of ^{157}Ta, while the third is much lower. The probability of an α particle escaping from the DSSD without depositing its full energy was measured to be ≈30% in this experiment and it is assumed that this is what happened to the ^{157}Ta α particle in this decay chain. In the correlation analysis, DSSD signals with recorded energies below 0.5 MeV were excluded, which means that the decays of ^{157}W were not considered because β particles generally deposited lower energies than this in the DSSD. The time intervals between the daughter and grand-daughter decays in all three cases are compatible with the reported half-lives of ^{157}W and states in ^{157}Ta. On the basis of this evidence, these decay chains are assigned as the α decays of the new nuclide ^{165}Pt. A further decay chain was assigned as a decay of ^{165}Pt and is presented in Table III. The daughter energy is interpreted as a ^{161}Os α particle that deposited only part of its energy, while the grand-daughter decay energy matches that of the ground state of ^{157}Ta. The full-energy α decays of all four ^{165}Pt decay chains are shown in Fig. 4(a).

An α-particle energy of 7272(14) keV was calculated for ^{165}Pt from the mean of the four decay chains, based on the energy calibration for data set A shown in Table II. It is interesting to note that the time interval between the recoil implantation and the ^{165}Pt α decay for the fourth decay chain is much shorter at 22 μs than the other 3, which are between 450 μs and 550 μs. However, analysis of the distribution of these four decay times using the method of Ref. [15] indicates that they are consistent with emanating from the same state. A half-life of $0.26^{+0.26}_{-0.09}$ ms was determined for ^{165}Pt from the four decay chains using the method of maximum likelihood [16] and correcting for a maximum time interval of 10 ms. This is much shorter than the predicted half-life for the β decay of ^{165}Pt [12], so it is assumed that the α-decay branching ratio is ≈100%.

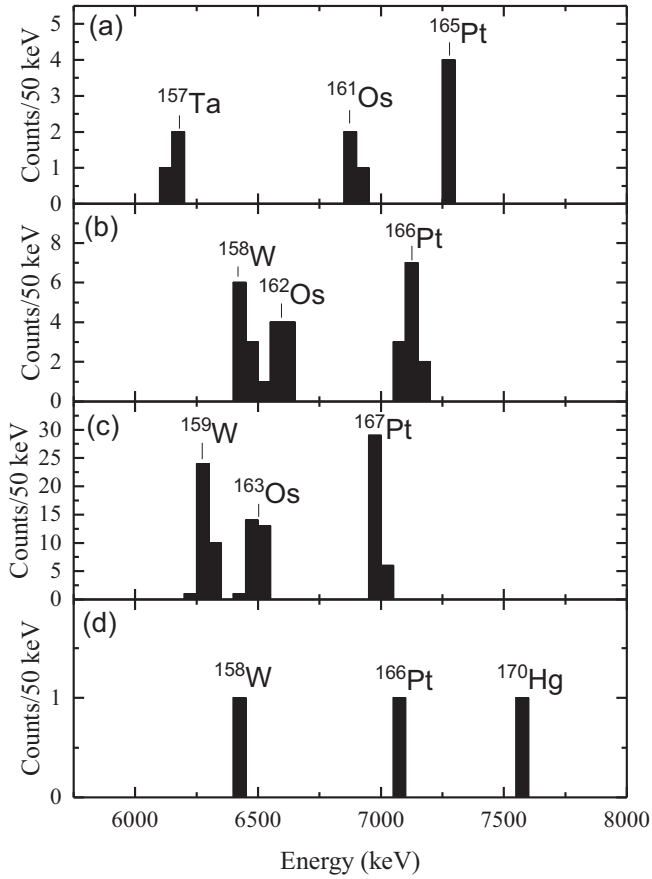

FIG. 4. Energy spectra of multiple correlated full-energy α decays for the decay chains of (a) ^{165}Pt, (b) ^{166}Pt, (c) ^{167}Pt, and (d) ^{170}Hg. The individual decay energies and time intervals for events in the ^{165}Pt chains are summarized in Table III.

B. Decays of ^{166,167}Pt

The isotopes ^{166,177}Pt were first identified by Bingham *et al.*, who used beams of 357 MeV and 384 MeV ^{78}Kr ions to bombard a ^{92}Mo target [4]. Data set A in the present work was obtained using the same beam and target combination, but at a significantly higher beam energy of 418 MeV. The fact that no decay chains of ^{166,167}Pt could be identified in data set A is probably a consequence of their production cross sections being much lower at this higher beam energy. However, decays of both these isotopes were identified in data sets B and C using the ^{96}Ru target, in which they were produced via αxn evaporation channels (see Fig. 2). In total, 11 decay chains of ^{166}Pt and 35 decay chains of ^{167}Pt were identified and their triple-correlated α decays are shown in Figs. 4(b) and 4(c), respectively. Figure 3(b) shows that daughter decay correlations were not sufficient to distinguish the decay chains of interest from other interfering activities from ^{171}Au in the case of ^{167}Pt and from ^{170}Au and ^{174}Hg in the case of ^{166}Pt. Grand-daughter correlations did allow clean separations to be made, and only double or better correlated events were accepted. For ^{166}Pt, an α-particle energy of 7118(8) keV and a half-life of $0.26^{+0.10}_{-0.06}$ ms were deduced from these decay chains, while the corresponding values for ^{167}Pt were 6985(8) keV and 1.1(2) ms, respectively. All values are in good agreement with those previously reported. The energy calibration for data sets B and C was based on the α decays shown in Table II.

TABLE II. The α-particle energies used to calibrate the DSSD α-particle energy spectra in the present work.

Data set A			Data sets B & C		
Nuclide	Energy (keV)	Ref.	Nuclide	Energy (keV)	Ref.
^{149}Tb	3967(3)	[10]	^{161}Ta	5148(5)	[10]
^{151}Dy	4069(3)	[10]	^{158}Hf	5269(4)	[7]
^{150}Dy	4236(2)	[10]	^{163}W	5384(2)	[10]
^{151}Ho	4521(3)	[10]	^{162}W	5534(3)	[10]
^{151}Ho^{m}	4607(3)	[10]	^{155}Lu	5578(4)	[11]
^{153}Er	4676(2)	[10]	^{168}Os	5676(4)	[10]
^{152}Er	4804(2)	[10]	^{167}Os	5836(2)	[10]
^{155}Lu^{m}	7390(5)	[7]	^{160}W	5912(5)	[7]
^{156}Hf^{m}	7782(4)	[7]	^{166}Os	6000(6)	[7]
			^{169}Ir	6126(5)	[10]
			^{168}Ir^{m}	6323(8)	[7]
			^{169}Pt	6678(15)	[6]

TABLE III. α-particle energies (E_α) and time intervals (τ) of all events observed in the ^{165}Pt decay chains, compared with literature values where available. Note that because the present experiment was not sensitive to β particles, the time interval between a given ^{161}Os α decay and its associated subsequent ^{157}Ta α decay represents the sum of the time interval between the ^{161}Os α decay and the ^{157}W β decay, and the time interval between this ^{157}W β decay and the ^{157}Ta α decay. α particles assumed to have escaped from the detector are indicated by italics.

Nuclide	E_α^1	E_α^2	E_α^3	E_α^4	E_α^{ref} (keV)
^{165}Pt	7267	7267	7286	7265	—
^{161}Os	6941	6872	6891	*2612*	6890(12) [13]
					6117(4) [14]
^{157}Ta	6158	6187	*2963*	6110	6213(4) [7]
Nuclide	τ^1	τ^2	τ^3	τ^4	$t_{1/2}^{\mathrm{ref}}$ (ms)
^{165}Pt	0.45	0.55	0.50	0.022	—
^{161}Os	2.2	1.35	1.0	1.4	0.64(6) [13]
^{157}W					275(40) [13]
					10.1(4) [14]
^{157}Ta	288	186	490	91	4.3(1) [7]

C. Decay of ^{170}Hg

Data sets B and C were searched for evidence of the expected α decay of ^{170}Hg [12]. A single candidate event chain was identified and is indicated in Fig. 3(b). The candidate ^{170}Hg α particle of energy 7590 keV occurred 0.12 ms after the implantation of a recoil into the same DSSD pixel and was followed by a sequence of particles with energies of 7065 keV, 1840 keV, and 6430 keV. This decay sequence is interpreted as the α decays of ^{166}Pt, ^{162}Os, and ^{158}W, where the ^{162}Os α particle did not deposit its full energy in the DSSD (see Fig. 2).

The time intervals between successive decays were 0.23 ms, 1.50 ms, and 3.35 ms, respectively, and are compatible with the reported half-lives of these α emitters [4,17]. Figure 4(d) shows α-particle energies of members of this triple-correlated decay chain. Using the method of maximum likelihood [16] and correcting for a 10 ms maximum time interval, a half-life of $0.08^{+0.40}_{-0.04}$ ms was deduced for the ^{170}Hg candidate event. As in the case of ^{165}Pt, this is much shorter than the predicted half-life for the β-decay branch [12], so it is assumed that the α-decay branching ratio is ≈100%.

D. Cross sections

Production cross sections were estimated from the measured yields of the nuclides of interest. The transport efficiency was simulated for each of the ions according to the different settings of MARA used during the experiment. The cross section for producing ^{170}Hg was estimated to be ≈0.5 nb in data set C, for which the beam energy was 390 MeV. This can be compared with the cross section of 4 nb reported by Bingham *et al.* for ^{166}Pt [4], which like ^{170}Hg in the present work, was produced via the 4*n* evaporation channel. The lower value found for ^{170}Hg could be a consequence of increased competition from fission in the de-excitation of the compound nucleus ^{174}Hg compared with ^{170}Pt.

The estimated cross section for the production of ^{165}Pt via the 5*n* evaporation channel was ≈0.7 nb. This continues the trend of decreasing cross sections with the increasing number of evaporated neutrons needed to produce isotopes that lie further from the line of β stability. The present cross section is consistent with the previously reported upper limit of 1 nb, albeit at a different beam energy [4]. The ^{166,167}Pt nuclei were produced via αxn evaporation channels in this work with cross sections at 390 MeV of 3.4 nb and 14 nb, and at 418 MeV (data set B) of 0.7 nb and 1.0 nb, respectively. The value for ^{166}Pt at 390 MeV is similar to that reported by Bingham *et al.* for production via the 4*n* evaporation channel, but the cross sections for ^{167}Pt at the beam energies used in the present work are lower than their value of 65 nb for the 3*n* channel [4]. There was no evidence in the present data for ^{165}Pt decay chains produced via the $\alpha 5n$ evaporation channel in data sets B or C.

IV. DISCUSSION

The measured α-particle energy for ^{165}Pt appears to continue the smooth systematic trend exhibited by its heavier isotopes, as can be seen in Fig. 5(a). The energy deduced for ^{170}Hg from the single decay chain fits well with the systematics of α-decay Q values for the ground states of Hg isotopes. Assuming that the full ^{170}Hg α-particle energy was registered, the reduced α-decay width determined using the method of Rasmussen [20] is 63^{+79}_{-53} keV. This value is compatible with those for α decays of other even-even nuclei in this region, see Fig. 6(a).

The corresponding value for ^{165}Pt is 33^{+23}_{-18} keV, while reduced decay widths of 90^{+23}_{-17} keV and 73^{+15}_{-12} keV were deduced for ^{166,167}Pt, respectively, from the averages of the α-particle energies and half-lives measured in the present work

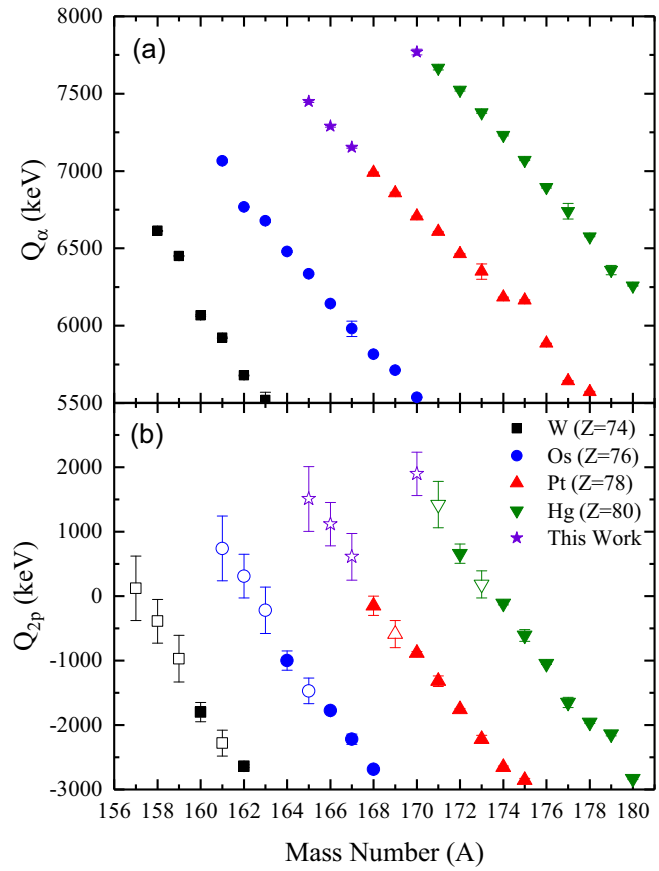

FIG. 5. The Q values for (a) α decay and (b) two-proton decay plotted as a function of mass number for isotopes of W, Os, Pt, and Hg [18,19]. Values that required a predicted mass to be used in the calculation are denoted by hollow markers, whereas values that use only directly measured masses have solid markers. In (a) the error bars are smaller than the plotted symbols.

and those reported by Bingham *et al.* [21]. These values are shown in Fig. 6(b). The value for ^{165}Pt is slightly lower than values determined for its heavier odd-*A* isotopes but appears to follow the trends of reducing decay widths with decreasing neutron number observed in lighter elements [22]. A similar trend has been identified above the $N = 126$ neutron shell closure and the $Z = 82$ shell closure and been attributed to reducing α-particle preformation probabilities [23,24]. When approaching shell closures, the α-particle preformation probability reduces due to there being fewer valence protons and neutrons, while further away from the shell closures nuclei are more deformed and α decays may therefore be faster [25–27]. Comparing the reduced α-decay width for ^{165}Pt with that of its nearest even-even neighbor, ^{166}Pt, yields a hindrance factor of 2.9, which is consistent with the α decay of ^{165}Pt being unhindered. This would suggest its ground state has the same spin and parity ($\frac{7}{2}^-$) as was proposed for the ground state of ^{161}Os [13].

Although both ^{165}Pt and ^{170}Hg are predicted to be unbound to the emission of two protons [12], values for their atomic masses, separation energies, etc., are not included in the 2016 Atomic Mass Evaluation [18,19]. However, it is possible to

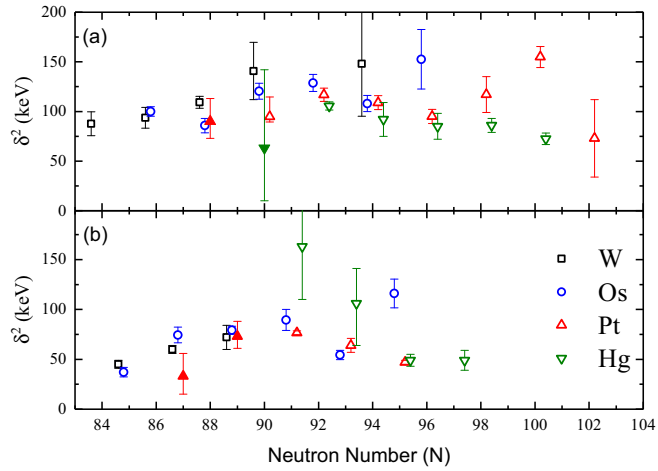

FIG. 6. Reduced α-decay widths of W, Os, Pt, and Hg nuclei calculated using the method of Rasmussen [20]. (a) shows values for even-A nuclei plotted as a function of neutron number, while (b) shows values for odd-A nuclei. The values for ^{170}Hg and ^{165,166,167}Pt are denoted by the solid symbols. Literature values for the other nuclides were taken from [10,11,21,29–36].

estimate their Q_{2p} values using the α-decay Q values determined in the present work combined with the evaluated two-proton separation energies of ^{161}Os and ^{166}Pt. The resulting values are shown in Fig. 5(b), from which it can be seen that these values continue the smooth trend of increasing Q_{2p} values with decreasing mass number for a given isotopic chain. Both new nuclides are two-proton unbound by more than 1 MeV, but both still decay primarily via α decay. The data were searched for evidence of two-proton decay candidate events, but none were found. The nonobservation is perhaps not surprising as in the work of Olsen *et al.* [28] it is predicted that two-proton decay will only begin to compete with α decay in ^{155}Pt and ^{159}Hg.

It seems improbable that such exotic nuclei could be observed using the same experimental methods as in the present work, because the cross sections are likely to be far too low. However, the cross sections may not be prohibitively small for the next nuclides beyond ^{165}Pt and ^{170}Hg. The smooth variation of α-decay Q values with mass number evident in Fig. 5(a) can be used to estimate how much further from stability one could probe before the half-lives drop below $\approx$1 μs, the typical time of flight through a recoil separator. If the trend continues, this lifetime threshold is likely to be crossed for Hg isotopes somewhere around ^{166}Hg. Similarly, for the Pt isotopes, $^{162-164}$Pt are probably all sufficiently long-lived to be observed although there was no evidence of α decays of ^{164}Pt in the present data. One could expect that the α-decay Q value departs from the smooth trend at the $N = 83$ nuclide ^{161}Pt as its α decay would involve breaking a closed neutron shell. It is likely that, similar to its heaviest known isotone ^{157}W, it mainly undergoes β decay and identifying these β decays will present additional experimental challenges.

ACKNOWLEDGMENTS

This work has been supported by the Academy of Finland under the Finnish Centre of Excellence Program (Contract No. 213503), the Academy of Finland (Grant No. 257562), the United Kingdom Science and Technology Facilities Council, the EU HORIZON2020 programme "Infrastructures" [Project No. 654002 (ENSAR2)], the Slovak Research and Development Agency (Contract No. APVV-15-0225), and by the Slovak grant agency VEGA (Contract No. 2/0129/17). J.H. acknowledges financial support from the University of Liverpool.

[1] R. J. Carroll, R. D. Page, D. T. Joss, J. Uusitalo, I. G. Darby, K. Andgren, B. Cederwall, S. Eeckhaudt, T. Grahn, C. Gray-Jones *et al.*, Phys. Rev. Lett. **112**, 092501 (2014).
[2] J. Sarén, The ion-optical design of the MARA recoil separator and absolute transmission measurements of the RITU gas-filled recoil separator, Ph.D. thesis, University of Jyväskyä, 2011.
[3] J. Uusitalo, J. Sarén, J. Partanen, and J. Hilton, Acta Phys. Pol. B. **50**, 319 (2019).
[4] C. R. Bingham, K. S. Toth, J. C. Batchelder, D. J. Blumenthal, L. T. Brown, B. C. Busse, L. F. Conticchio, C. N. Davids, T. Davinson, D. J. Henderson, R. J. Irvine, D. Seweryniak, W. B. Walters, P. J. Woods, and B. E. Zimmerman, Phys. Rev. C **54**, R20 (1996).
[5] H. Kettunen, T. Enqvist, T. Grahn, P. T. Greenlees, P. Jones, R. Julin, S. Juutinen, A. Keenan, P. Kuusiniemi, M. Leino *et al.*, Phys. Rev. C **69**, 054323 (2004).
[6] S. Hofmann, G. Münzenberg, F. Heßberger, W. Reisdorf, P. Armbruster, and B. Thuma, Z. Phys. A **299**, 281 (1981).
[7] R. D. Page, P. J. Woods, R. A. Cunningham, T. Davinson, N. J. Davis, A. N. James, K. Livingston, P. J. Sellin, and A. C. Shotter, Phys. Rev. C **53**, 660 (1996).
[8] I. H. Lazarus, D. E. Appelbe, P. A. Butler, P. J. Coleman-Smith, J. R. Cresswell, S. J. Freeman, R. D. Herzberg, I. Hibbert, D. J. Joss, S. C. Letts *et al.*, IEEE Trans. Nucl. Sci. **48**, 567 (2001).
[9] P. Rahkila, Nucl. Instrum. Methods Phys. Res. A **595**, 637 (2008).
[10] A. Rytz, At. Data Nucl. Data Tables **47**, 205 (1991).
[11] S. Hofmann, P. Armbruster, G. Berthes, T. Faestermann, A. Gillitzer, F. P. Heßberger, W. Kurcewicz, G. Münzenberg, K. Poppensieker, H. J. Schott *et al.*, Z. Phys. A **333**, 107 (1989).
[12] P. Möller, J. Nix, and K.-L. Kratz, At. Data Nucl. Data Tables **66**, 131 (1997).
[13] L. Bianco, R. D. Page, I. Darby, D. Joss, J. Simpson, J. Al-Khalili, A. Cannon, B. Cederwall, S. Eeckhaudt, S. Ertürk *et al.*, Phys. Lett. B **690**, 15 (2010).
[14] R. J. Irvine, C. N. Davids, P. J. Woods, D. J. Blumenthal, L. T. Brown, L. F. Conticchio, T. Davinson, D. J. Henderson, J. A. Mackenzie, H. T. Penttilä *et al.*, Phys. Rev. C **55**, R1621 (1997).
[15] K. Schmidt, Eur. Phys. J. A **8**, 141 (2000).
[16] K. Schmidt, C.-C. Sahm, K. Pielenz, and H.-G. Clerc, Z. Phys. A **316**, 19 (1984).

[17] H. Mahmud, C. N. Davids, P. J. Woods, T. Davinson, D. J. Henderson, R. J. Irvine, D. Seweryniak, and W. B. Walters, Phys. Rev. C **62**, 057303 (2000).
[18] W. Huang, G. Audi, M. Wang, F. G. Kondev, S. Naimi, and X. Xu, Chin. Phys. C **41**, 030002 (2017).
[19] M. Wang, G. Audi, F. G. Kondev, W. Huang, S. Naimi, and X. Xu, Chin. Phys. C **41**, 030003 (2017).
[20] J. O. Rasmussen, Phys. Rev. **113**, 1593 (1959).
[21] C. R. Bingham, M. B. Kassim, M. Zhang, Y. A. Akovali, K. S. Toth, W. D. Hamilton, H. K. Carter, J. Kormicki, J. von Schwarzenberg, and M. M. Jarrio, Phys. Rev. C **51**, 125 (1995).
[22] A. N. Andreyev, M. Huyse, P. Van Duppen, C. Qi, R. J. Liotta, S. Antalic, D. Ackermann, S. Franchoo, F. P. Heßberger, S. Hofmann, I. Kojouharov, B. Kindler, P. Kuusiniemi, S. R. Lesher, B. Lommel, R. Mann, K. Nishio, R. D. Page, B. Streicher, S. Saro, B. Sulignano, D. Wiseman, and R. A. Wyss, Phys. Rev. Lett. **110**, 242502 (2013).
[23] C. Xu, G. Röpke, P. Schuck, Z. Ren, Y. Funaki, H. Horiuchi, A. Tohsaki, T. Yamada, and B. Zhou, Phys. Rev. C **95**, 061306(R) (2017).
[24] C. Qi, Rev. Phys. **1**, 77 (2016).
[25] D. L. Hill and J. A. Wheeler, Phys. Rev. **89**, 1102 (1983).
[26] D. S. Delion, A. Insolia, and R. J. Liotta, Phys. Rev. C **49**, 3024 (1994).
[27] N. Severijns, A. A. Belyaev, A. L. Erzinkyan, P.-D. Eversheim, V. T. Filimonov, V. V. Golovko, G. M. Gurevich, P. Herzog, I. S. Kraev, A. A. Lukhanin *et al.*, Phys. Rev. C **71**, 044324 (2005).
[28] E. Olsen, M. Pfützner, N. Birge, M. Brown, W. Nazarewicz, and A. Perhac, Phys. Rev. Lett. **110**, 222501 (2013).
[29] D. T. Joss, K. Lagergren, D. E. Appelbe, C. J. Barton, J. Simpson, B. Cederwall, B. Hadinia, R. Wyss, S. Eeckhaudt, T. Grahn *et al.*, Phys. Rev. C **70**, 017302 (2004).
[30] M. Sandzelius, E. Ganioğlu, B. Cederwall, B. Hadinia, K. Andgren, T. Bäck, T. Grahn, P. Greenlees, U. Jakobsson, A. Johnson, P. M. Jones, R. Julin, S. Juutinen, S. Ketelhut, A. Khaplanov, M. Leino, M. Nyman, P. Peura, P. Rahkila, J. Sarén, C. Scholey, J. Uusitalo, and R. Wyss, Phys. Rev. C **79**, 064315 (2009).
[31] M. Venhart, A. N. Andreyev, S. Antalic, L. Bianco, P. T. Greenlees, U. Jakobsson, P. Jones, D. T. Joss, R. Julin, S. Juutinen *et al.*, Eur. Phys. J. A **48**, 101 (2012).
[32] H. Badran, C. Scholey, K. Auranen, T. Grahn, P. T. Greenlees, A. Herzan, U. Jakobsson, R. Julin, S. Juutinen, J. Konki *et al.*, Phys. Rev. C **94**, 054301 (2016).
[33] K. S. Toth, C. R. Bingham, J. C. Batchelder, L. T. Brown, L. F. Conticchio, C. N. Davids, R. J. Irvine, D. Seweryniak, D. M. Moltz, W. B. Walters, J. Wauters, and E. F. Zganjar, Phys. Rev. C **60**, 011302(R) (1999).
[34] Y. Akovali, Nucl. Data Sheets **84**, 1 (1998).
[35] A. Demin, T. Fényes, I. Mahunka, V. Subbotin, and L. Trón, Nucl. Phys. A **106**, 337 (1967).
[36] A. Siivola, Nucl. Phys. **84**, 385 (1966).